Res Chem Intermed
DOI 10.1007/s11164-016-2590-z

Preparation of immobilized hexamine on Fe_3O_4/SiO_2 core/shell nanoparticles: a novel catalyst for solvent-free synthesis of bis(indolyl)methanes

Sahar Kangari[1] · Issa Yavari[2]

Received: 3 February 2016 / Accepted: 23 May 2016

Abstract Hexamethylenetetramine covalently immobilized on silica-coated magnetic nanoparticles is prepared and characterized by XRD, FT-IR, SEM, and VSM. According to SEM pictures, the nanoparticles are mostly spherical in shape, and their size is approximately 46 nm. The catalytic performance of these magnetic nanoparticles for the synthesis of bis(indolyl)methanes was investigated. The catalyst was readily recycled by the use of an external magnetic field and can be reused four times without significant loss of activity.

Graphical Abstract

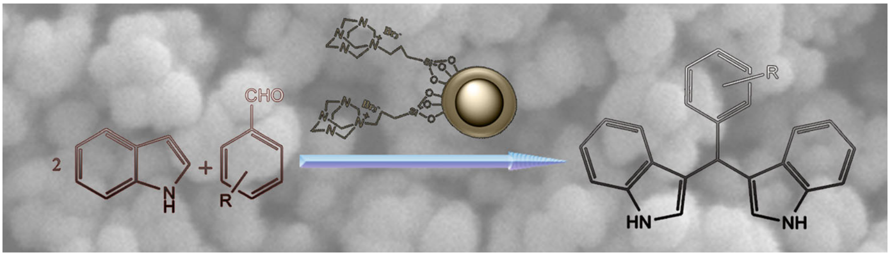

Keywords Magnetically retrievable · Nano-hybrid · Bis(indolyl)methanes · Solvent-free · Silica · Hexamethylenetetramine

---

✉ Issa Yavari
yavarisa@modares.ac.ir

[1] Department of Chemistry, Science and Research Branch, Islamic Azad University, Tehran, Iran

[2] Chemistry Department, Tarbiat Modares University, PO Box 14115-175, Tehran, Iran

Introduction

Catalytic applications of magnetic nanoparticles (MNPs) have attracted increasing attention owing to their unique magnetic properties and easy separation from the reaction system by an external magnetic field rather than filtration or centrifugation [1–5]. However, MNPs without coating are often unstable and tend to aggregate during catalytic transformations, resulting in a remarkable drop of catalytic activity owing to the decrease of surface area. Thus, MNPs are modified with high surface coating materials. Silica is usually used as an important coating material because of its low cost, high surface area, and ease of modification with organic functional groups [6]. Recently, silica-coated MNPs have been used as appropriate supports for covalent bond formation with organic materials [7–9].

Indole and its derivatives are an important class of heterocyclic compounds in medicinal chemistry. In particular, bis(indolyl)methanes (BIMs) are active against human cancer cells [10–13]. The electrophilic substitution reaction of indoles with aldehydes affords the corresponding BIMs. Many of these methods still suffer from drawbacks, for example, expensive reagents, long reaction time, low yields, corrosive reagents, and high catalyst loading, which eventually results in the generation of large amounts of toxic waste [14–16]. Therefore, there is a need for an efficient, recyclable, and eco-friendly catalyst for the synthesis of BIMs.

Herein, we report a synthesis of novel core–shell MNPs having a spherical shape as a core and porous silica as a shell that is modified with HMTA tribromide. This Fe_3O_4–SiO_2–HMTA tribromide is used as a heterogeneous nanocatalyst for the synthesis of BIMs by condensation of indole with aldehydes and ketones.

Experimental

Materials and methods

Iron(III) chloride hexahydrate ($FeCl_3 \cdot 6H_2O$), Iron(II) chloride tetrahydrate ($FeCl_2 \cdot 4H_2O$), ammonium hydroxide solution ($NH_3 \cdot H_2O$, 25 %), tetraethyl orthosilicate (TEOS), 3-chloropropyltrimethoxysilane (CPTMS), hexamethylenetetramine (hexamine, HMTA), KBr, Br_2, indole, aldehydes, and solvents were obtained from Merck.

Fabrication of the catalyst

Synthesis of MNPs

MNPs were prepared by co-precipitation method [17]. Therefore, a solution of $FeCl_2 \cdot 4H_2O$ (1.27 g) in deionized water (25 mL) was added to a solution of $FeCl_3 \cdot 6H_2O$ (3.80 g) in deionized water (25 mL), and the resulting solution was vigorously stirred. Then, 10 mL of ammonia (25 %) was added dropwise into the solution and stirred at 80 °C for 2 h. When the black precipitate was formed, the upper solution was discarded and the precipitate was washed several times with deionized ethanol and dried.

Synthesis of citrate-coated Fe_3O_4 MNPs

For the preparation of citrate-coated iron oxide, 1.0 g of Fe_3O_4 MNPs was added to 30 mL of 0.1 M citric acid, sonicated for 30 min, and stirred under N_2 for 12 h. Then, the coated MNPs were separated by external magnet and washed twice with deionized water and dried.

Synthesis of Fe_3O_4–SiO_2NPs

The silica-coated magnetic NPs were prepared by coating of silica layer [18]. For this purpose, the obtained CMNPs were added to the solution containing 20 mL of ethanol and 4 mL of deionized water and sonicated for 30 min. Then, ammonium hydroxide (5 mL) was added followed by 2 mL of TEOS and stirred under N_2 for 2 h. The obtained precipitate was washed by ethanol several times and dried in an oven.

Synthesis of Fe_3O_4–SiO_2–CPTMS

The obtained silica-coated magnetic NPs were dispersed in the solution containing 100 mL of ethanol and 2 mL of toluene and then sonicated for 30 min. Next, 2 mL of CPTMS was added to the resulting solution, and stirred under N_2 for 48 h. In the last stage, the resulting precipitate washed several times by methanol and dried.

Synthesis of Fe_3O_4–SiO_2–HMTA

A stirred suspension of hexamine (1.40 g) and the synthesized Fe_3O_4–SiO_2–CPTMS in $CHCl_3$ was refluxed at 60 °C for 24 h. The resulting brown precipitate was washed twice by $CHCl_3$ and dried under vacuum at 80 °C.

Modification of immobilized hexamine by exchanging chloride with tribromide

For exchange of the chloride counter ion with bromide ion, the precipitate was stirred with a saturated KBr solution for 48 h. Finally, HMTA bromide salt immobilized on silica was treated with Br_2 (1 mL) and diluted in CH_2Cl_2 (10 mL) to afford the final HMTA tribromide silica support catalyst (Scheme 1).

Identification of the catalyst

Scanning electron microscope (SEM) images were obtained using a LEO 1430VP instrument. FT-IR spectra of the materials were recorded over the range of 400–4000 cm^{-1} region by using a Bruker Tensor 27 series FT-IR spectrometer.

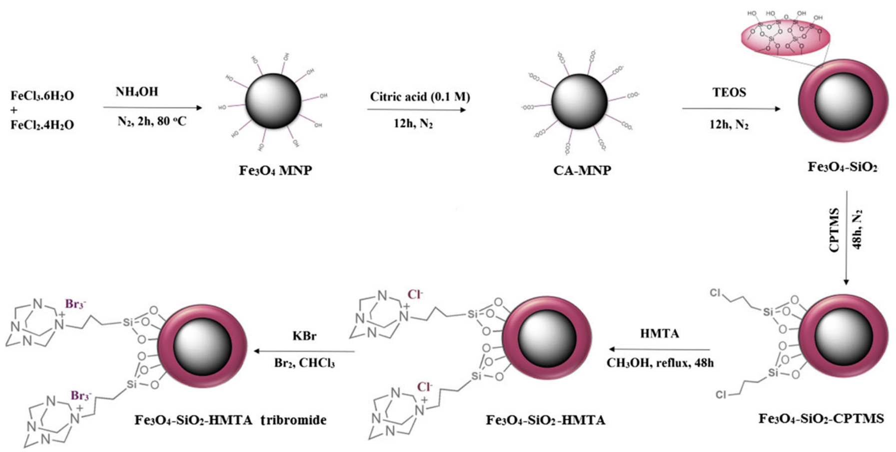

Scheme 1 Schematic representation of the synthesis of Fe_3O_4–SiO_2–HMTA tribromide

Using the KBr disc method with a 1 % sample in 200 mg of spectroscopic-grade KBr. Powder X-ray diffraction (XRD) patterns were recorded in the range of 2°–70° on a Siemens D5000 X-ray diffractometer, using CuKα radiation ($\lambda = 1.5418$ Å) at 30 kV and 30 mA. The magnetic studies were carried out on a VSM Lake Shore 7307 Vibrating Sample Magnetometer.

Catalytic applications of Fe_3O_4–SiO_2–HMTA tribromide for the synthesis of BIMs

A mixture of aldehyde or ketone (1 mmol), indole (2 mmol), and catalyst (0.01 g) was stirred at 80 °C for 10 min. The reaction was monitored by TLC. After completion of the reaction, EtOH (3 mL) was added and the catalyst was separated by an external magnet. In the recycling experiment, the separated catalyst was then washed with ethanol and dried in oven to remove residual solvent. The results of synthesis of BIMs under solvent-free conditions at 80 °C, are presented in Table 1.

Spectral data of selected compounds

3-[(1H-Indol-3-yl)(phenyl)methyl]-1H-indole **(3a)** Mp 150–154 °C; IR (KBr, cm^{-1}): 3407, 3049, 2845, 1597, 1451, 740, 588; ^1H NMR (400 MHz, DMSO-d_6): δ 5.94 (s, 1 H, CH), 6.53 (d, ^3J 1.6 Hz, 2 H, 2 CH), 7.08 (t, 2 H, 2 CH), 7.28–7.36 (m, 7 H, 7 CH), 7.4 (d, ^3J 7.6 Hz, 2 H, 2 CH), 7.46 (d, ^3J 7.9 Hz, 2 H, 2 CH), 7.5 (s, 2 H, 2 NH).

3-[(1H-indol-3-yl)(p-tolyl)methyl]-1H-indole **(3b)** Mp 96–99 °C; IR (KBr, cm^{-1}): 3408, 3044, 2839, 1508, 1451, 1004, 742, 588, 472; ^1H NMR (400 MHz, DMSO-d_6): δ 2.23 (s, 3 H, Me), 5.79 (s, 1 H, CH), 6.49 (d, ^3J 1.6 Hz, 2 H, 2 CH), 6.96 (t, ^3J 7.1, 7.7 Hz, 2H, 2 CH), 7.04 (d, ^3J 7.8 Hz, 2 H, 2 CH), 7.12 (t, 2 H, 2 CH), 7.17–7.23 (m, 4 H, 4 CH), 7.36 (d, ^3J 7.9 Hz, 2 H, 2 CH), 7.58 (s, 2 H, 2 NH).

Table 1 Synthesis of bis(indolyl)methanes **3** catalyzed by Fe_3O_4–SiO_2–HMTA tribromide

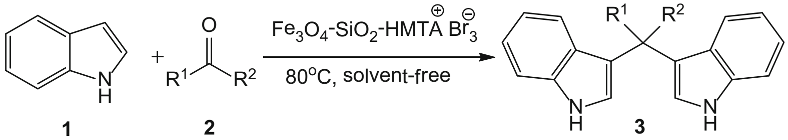

Entry	R^1	R^2	Product	Yield (%)	Mp (°C) Observed	Mp (°C) Reported
1	Ph	H	**3a**	97	150–154	150–152 [20]
2	4-Me-C_6H_4	H	**3b**	93	96–99	94–96 [20]
3	4-MeO-C_6H_4	H	**3c**	91	187–191	187–189 [20]
4	4-HO-C_6H_4	H	**3d**	96	120–124	120–123 [21]
5	4-O_2N-C_6H_4	H	**3e**	94	219–223	219 [21]
6	4-Cl-C_6H_4	H	**3f**	93	74–77	76–77 [20]
7	3-Me-C_6H_4	H	**3g**	94	95–99	97–99 [25]
8	3-MeO-C_6H_4	H	**3h**	93	184–188	187–180 [25]
9	3-HO-C_6H_4	H	**3i**	95	132–135	136–139 [21]
10	3-O_2N-C_6H_4	H	**3j**	93	262–265	217–221 [20]
11	3-Cl-C_6H_4	H	**3k**	92	71–75	74 [20]
12	2-Me-C_6H_4	H	**3l**	93	90–94	95–97 [21]
13	2-MeO-C_6H_4	H	**3m**	96	132–135	134–136 [21]
14	2-HO-C_6H_4	H	**3n**	94	130–135	134–137 [25]
15	2-O_2N-C_6H_4	H	**3o**	94	138–142	137–139 [21]
16	2-Cl-C_6H_4	Me	**3p**	92	105–107	107–109 [21]
17	Ph	H	**3q**	91	186–188	189–190 [23]
18	cHex	H	**3r**	93	116–119	118–120 [23]
19	Me	H	**3s**	92	91–94	94–97 [22]
20	^{n}Pent	H	**3t**	92	63–66	67–71 [26]
21	^{n}Pr	H	**3u**	93	115–119	118–120 [21]
22	^{n}Bu	H	**3v**	92	74–78	72–74 [27]
23	H	H	**3w**	90	148–153	150 [22]
24	Me	Me	**3x**	92	63–67	66–69 [23]

Reaction time = 10 min

3-[(1H-indol-3-yl)(4-methoxyphenyl)methyl]-1H-indole **(3c)** Mp 187–191 °C; IR (KBr, cm^{-1}): 3394, 3054, 2356, 1666, 1605, 1455, 1235, 749; ^1H NMR (400 MHz, DMSO-d_6): δ 3.76 (s, 3 H, MeO), 5.82 (s, 1 H, CH), 6.60 (d, ^3J 1.5 Hz, 1 H, 2 CH), 6.71–6.82 (m, 2 H, 2 CH), 7.13–7.17 (m, 2 H, 2 CH), 7.3 (d, ^3J 8.1, 2 H, 2 CH), 7.3 (d, ^3J 7.9, 2 H, 2 CH), 7.88 (s, 2 H, 2 NH).

3-[(1H-indol-3-yl)(4-nitrophenyl)methyl]-1H-indole **(3e)** Mp 219–223 °C; IR (KBr, cm^{-1}): 3442, 3052, 1592, 1502, 1341, 1502, 1454, 1341, 733, 512; ^1H NMR (400 MHz, DMSO-d_6) δ 5.99 (s, 1 H, CH), 6.69 (d, ^3J 8.0 Hz, 1 H, 2 CH), 7.01–7.05 (m, 2 H, 2 CH), 7.18–7.20 (m, 2 H, 2 CH), 7.34 (d, ^3J 7.9 Hz, 2 H, 2 CH), 7.39 (d, ^3J 8.1 Hz, 2 H, 2 CH), 7.51 (d, ^3J 8.6 Hz, 2 H, 2 CH), 8.02 (s, 2 H, 2 NH), 8.14 (dd, ^3J 6.9 Hz, 2H, 2 CH).

Results and discussion

Preparation of the catalyst

The magnetic nanoparticles were easily prepared via the co-precipitation method [24]. Citric acid was used as a coating agent, covalently attached on the MNPs surface, and made stable colloidal dispersion. The choice of citric acid over other commonly available coating agents is to control the hydrodynamic size and prevent aggregation of MNPs at physiological condition, coating the magnetic nanoparticles with the silica matrix should be a good solution. Furthermore, the silica hydroxyl groups (Si–OH) were modified by CPTMS groups with covalent bonds. Finally, HMTA was immobilized on the nanoparticle with covalent bonds between Silane groups and HMTA.

Characterization of the catalyst

The Fourier transform infrared (FT-IR) spectra of (a) Fe_3O_4, (b) Fe_3O_4–SiO_2, and (c) Fe_3O_4–SiO_2–HMTA tribromide are shown in Fig. 1. The FT-IR spectrum of MNPs (Fig. 1a) the absorption bands around 3438 cm^{-1} is attributed to the stretching vibrations of hydroxyl group absorbed by MNPs and the peak at 1613 cm^{-1} is assigned to the hydroxyl bending. The absorption band at 565 cm^{-1} is attributed to the Fe–O bond vibration of magnetite [17]. The broad high-intensity band at 1062 cm^{-1} in spectrum of Fe_3O_4–SiO_2 (Fig. 1b) is assigned to the asymmetric stretching bands of Si–O–Si in silica shell. The band at 799 cm^{-1} is assigned to the Si–O–Si symmetric stretch, while the band at 455 cm^{-1} corresponds to vibration of the silicate ring structure. The band at 956 cm^{-1} is assigned to the Si–O stretch. The bands at 3425, 1630 cm^{-1} correspond to the stretching and

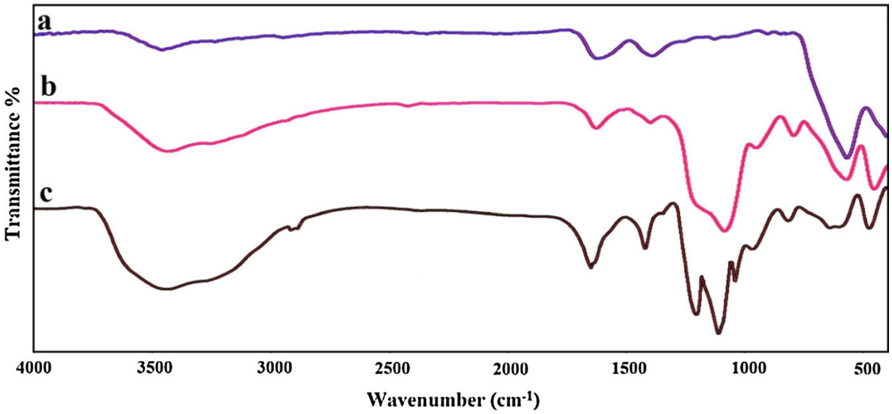

Fig. 1 FT-IR spectra of (*a*) Fe_3O_4, (*b*) Fe_3O_4–SiO_2 , and (*c*) Fe_3O_4–SiO_2–HMTA tribromide

bending vibrations of Si–OH [18]. The IR spectrum shown in Fig. 1c demonstrates the characteristic bands of organic group modified on the Fe_3O_4–SiO_2 framework. There are two characteristic bands including C–H stretching 2925 and 2999 cm^{-1} and bending bonds at, 1459 and 1374 cm^{-1} of the hexamine ring and CPTMS, C–N^+ stretching at 1615 cm^{-1} [19]. Stretching bonds of the C–N moiety are at 1009–1233 cm^{-1}. The band around 1628 cm^{-1} is due to the bending vibration of the hydroxyl groups of silica.

Furthermore, tribromide was characterized by biamperometric titration method. Generally, amperometric titrations can be carried out with relatively simple equipment. In this work, the platinum wire was used as an electrode. The reference electrode can be double-compartmented with the Ag/AgC1 (3M KC1) reference in the inner compartment and an appropriate electrolyte solution in the outer, the outer being in contact with both the reference and the solution under investigation. The analyte should be held in a titration vessel of 50–100 mL capacity. With the availability of advanced electronic instrumentation, including microprocessor- or computer-controlled titrators with microburettes, amperometric titrations are carried out on a more or less automatic basis. This is particularly true of biamperometric titrations. The auxiliary equipment required to convert the usual modern potentiometric titrator into one capable of amperometric titration involves a unit called a "polarizer". This unit, linked to the potentiometric titration unit, provides the fixed applied potential required. It can also set the limit within which the current is expected to fall during the titration. The current changes are converted to mV values and the titrator plots these values against the titrant volume. The polarizer/titrator combination can also be used in dead-stop titrations to stop the titration at a current representative of the endpoint. Polarizers are also capable of carrying out titrations by fixing the current allowed to flow and then plotting the potential changes required to sustain this current flow against titrant volume. Here again, this mode can be used to permit dead-stop titrations to be carried out.

All of the observed diffraction peaks are indexed by the cubic structure of Fe_3O_4 (PDF: 00-011-0614). As can be seen, the XRD pattern of Fe_3O_4–SiO_2–HMTA tribromide organic–inorganic hybrid nanomaterial is in agreement with that of the standard magnetite (Fe_3O_4) structure. Thus, the particles have phase stability and their structural integrity is preserved. The diffraction peaks at $2\theta = 29.9$, 35.4, 43.1, 53.4, 57.3, 62.4, and 74.1 correspond to the (2 2 0), (3 1 1), (4 0 0), (4 2 2), (5 1 1), (4 4 0), and (5 3 3) of Fe_3O_4 crystalline structure (Fig. 2).

To have a better insight into the morphology of magnetite and Fe_3O_4–SiO_2–HMTA tribromide and composite structural changes, scanning electron microscopy images were observed. Figure 3a clearly shows the Fe_3O_4 NPs with uniform structures. Moreover, as shown in Fig. 3b, the Fe_3O_4–SiO_2–HMTA tribromide organic–inorganic hybrid nanomaterials have core–shell NPs.

The magnetic properties of Fe_3O_4 were characterized by vibrating sample magnetometer (VSM). The typical room temperature magnetization curves of bare Fe_3O_4 (Fig. 4a) and Fe_3O_4–SiO_2–HMTA tribromide (Fig. 4b) are shown. The magnetic saturation values of the Fe_3O_4 and Fe_3O_4–SiO_2–HMTA were 69 and 32 emu/g, respectively. The lower magnetic saturation of later NPs may be attributed to the existence of nonmagnetic materials on the surface of MNPs.

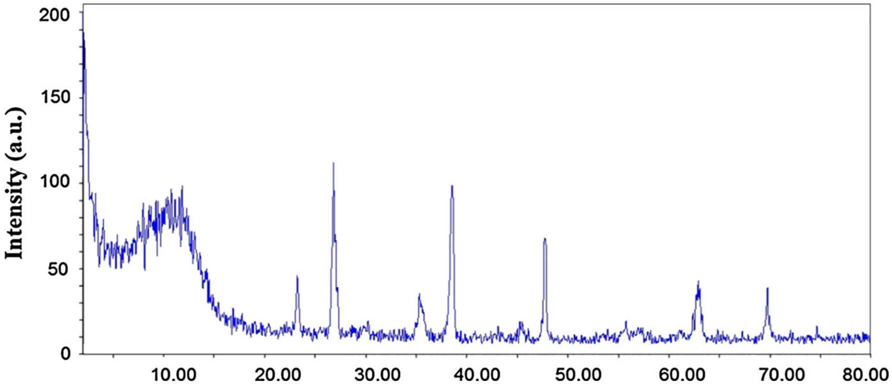

Fig. 2 The XRD powder diffraction patterns of Fe_3O_4–SiO_2–HMTA tribromide

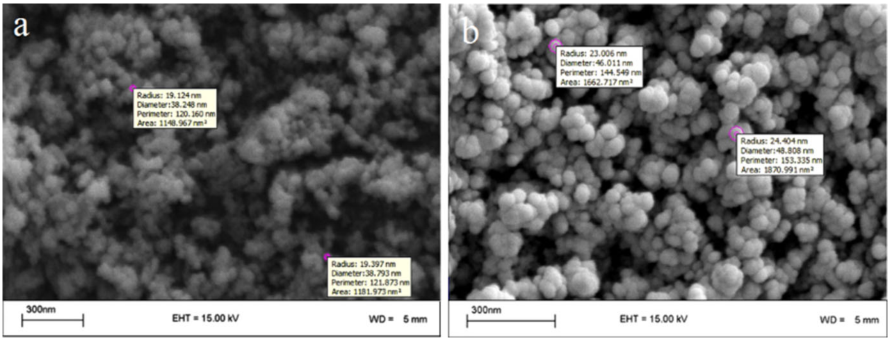

Fig. 3 The SEM images of **a** Fe_3O_4 and **b** Fe_3O_4–SiO_2–HMTA tribromide

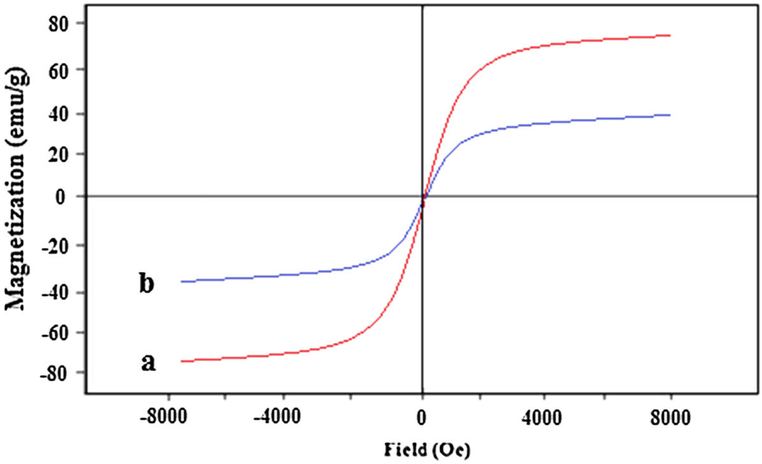

Fig. 4 Magnetization curves obtained by VSM at room temperature for **a** Fe_3O_4 MNPs and **b** Fe_3O_4–SiO_2–HMTA tribromide

Table 2 A comparison between this work and similar works for the synthesis of 3-[(1*H*-indol-3-yl)(phenyl)methyl]-1*H*-indole (**3a**)

Entry	Reagent and conditions	Time	Yield (%)	References
1	Nano-TiO_2, Solvent-free, 80 °C	30 min	95	[22]
2	$ZrOCl_2 \cdot 8H_2O$, Solvent-free, 50 °C	40 min	84	[28]
3	$In(OTf)_3/CH_3CN$	25 min	71	[29]
4	$La(PFO)_3$/EtOH	30 min	90	[30]
5	Alum 100 °C	60 min	73	[29]
6	$ZrCl_4CH_3CN$	35 min	91	[31]
7	[bmim] [Br] None r.t.	8	50	[32]
8	HPA/TPI-Fe_3O_4, Solvent-free/100 °C	25 min	96	[33]
9	HPA/TPI-SBA-15, Solvent-free/100 °C	15 min	84	[34]
10	Fe_3O_4–SiO_2–HMTA tribromide, Solvent-free/80 °C	10 min	96	This work

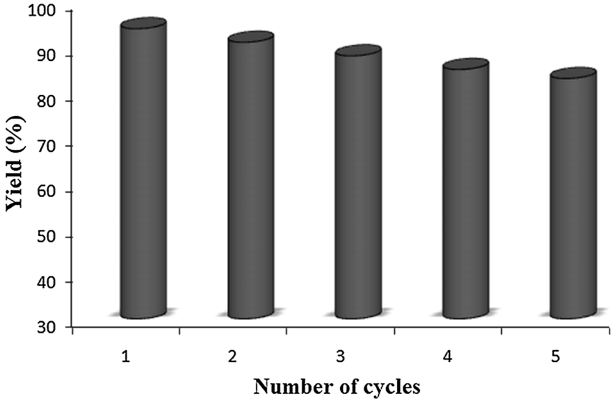

Fig. 5 Recyclability of Fe_3O_4–SiO_2–HMTA tribromide determined for the synthesis of **3a**

The superiority of the present protocol over reported methods can be seen by comparing our results with those of some recently reported procedures, as shown in Table 2. The synthesis of 3-[(1*H*-indol-3-yl)(phenyl)methyl]-1*H*-indole (**3a**) was used as a model reaction and the comparison is in terms of mol% of the catalysts, temperature, reaction time, and yields.

The efficiency of the catalyst was determined for the synthesis of compound **3a**. As shown in Fig. 5, after four times recycling, the yield was reduced to 85 %.

Conclusions

In summary, the surface of silica-coated magnetite NPs has been modified with 3-chloropropyltrimethoxysilane groups (CPTMS), then for the first time, surface of silica-coated magnetic NPs has been modified with covalently immobilized between the hexamine and the silane groups. This novel catalyst was characterized by XRD, FTIR, SEM, and VSM. The research found that Fe_3O_4–SiO_2–HMTA tribromide is an appropriate nanomagnetic catalyst with a high stability for the synthesis of BIMs under solvent-free conditions. This nanocatalyst also was found to be very stable after four times reusability. The nanomagnetic catalyst can also be readily separated from reaction systems by external magnetic field.

References

1. S. Laurent, D. Forge, M. Port, A. Roch, C. Robic, L.V. Elst, R.N. Muller, Chem. Rev. **108**, 2064 (2008)
2. S.G. Kwon, T. Hyeon, Acc. Chem. Res. **41**, 1696 (2008)
3. L. Adak, K. Chattopadhyay, B.C. Ranu, J. Org. Chem. **74**, 3982 (2009)
4. V. Polshettiwar, B. Baruwati, R.S. Varma, Green Chem. **11**, 127 (2009)
5. F. Shirini, M.S. Langroodi, M. Abedini, Chin. Chem. Lett. **21**, 1342 (2010)
6. J.A. Howarter, J.P. Youngblood, Langmuir **22**, 11142 (2006)
7. A. Rostami, Y. Navasi, D. Moradi, AGh Choghamarani, Catal. Commun. **43**, 16 (2014)
8. G.M. Ucoski, F.S. Nunes, G.D. Silva, Y.M. Idemori, Sh Nakagaki, Appl. Catal. A **459**, 121 (2013)
9. A. Ying, Sh Liu, Y. Ni, F.S. Xu, W. Tang, Catal. Sci. Technol. **4**, 2115 (2014)
10. F. Shirini, M. Abedini, J. Nanosci. Nanotechnol. **13**, 4838 (2013)
11. F.K. Behbahani, M. Sasani, J. Serb. Chem. Soc. **77**, 1157 (2012)
12. C. Hong, G.L. Firestone, L.F. Bjeldanes, Biochem. Pharmacol. **63**, 1085 (2002)
13. T.R. Garbe, M. Kobayashi, N. Shimizu, N. Takesue, M. Ozawa, H. Yukawa, J. Nat. Prod. **63**, 596 (2002)
14. R. Nagarajan, P.T. Perumal, Chem. Lett. **33**, 288 (2004)
15. M. Chakrabarty, A. Mukherji, S. Karmakar, S. Arims, Y. Harigaya, Heterocycles **68**, 331 (2006)
16. M. Chakrabarty, R. Mukherjee, A. Mukherji, S. Arims, Y. Harigaya, Heterocycles **68**, 1659 (2006)
17. M. Benelmekki, C. Caparros, A. Montras, R. Gonçalves, S. Lanceros-Mendez, L.M. Martinez, J. Nanopart. Res. **13**, 3199 (2011)
18. Y. Yunjin, M. Shiding, Y. Shaoming, M. Ping, S. Hongqi, W. Shaobin, J. Colloid Interface Sci. **379**, 20 (2012)
19. S. Lucarini, M. Mari, G. Piersanti, G. Spadoni, RSC Adv. **3**, 19135 (2013)
20. P.J. Das, J. Das, Tetrahedron Lett. **35**, 4718 (2012)
21. A.K. Chakraborti, S.R. Roy, D. Kumar, P. Chopra, Green Chem. **10**, 1111 (2008)
22. M. Karthik, C.J. Magesh, P.T. Perumal, M. Palanichamy, Appl. Catal. A Gen. **286**, 137 (2005)
23. S.B. Sapkal, K.F. Shelke, B.B. Shingate, M.S. Shingare, Bull. Korean Chem. Soc. **31**, 351 (2010)
24. S. Sobhani, Z. Pakdin, R. Nasseri, J. Chem. Sci. **125**, 975 (2013)
25. M. Rahimizadeh, Z. Bakhtiarpoor, H. Eshghi, M. Pordel, Gh Rajabzadeh, Monatsh. Chem. **140**, 1465 (2009)
26. S.S. Ekbote, M.K. Deshmukh, Z.S. Qureshi, B.M. Bhanage, Catal. Lett. **128**, 418 (2009)
27. H.J. Grambow, G. Garden, F. Dallacker, A. Lehmann, Zeitsch. Pflanzenphysiol **82**, 62 (1977)
28. H. Firouzabadi, N. Iranpoor, M. Jafarpour, A. Ghaderi, J. Mol. Cat. A. Chem. **253**, 249 (2006)
29. R. Nagarajan, P.T. Peruma, Tetrahedron **58**, 1229 (2002)
30. L. Wang, J. Han, H. Tian, J. Sheng, Z. Fan, X. Tang, Synlett 337 (2005)
31. S. Sobhani, R. Jahanshahi, New J. Chem. **37**, 1009 (2013)
32. A. Kumar, P. Kumar, V.D. Tripathia, S. Srivastavaa, RSC Adv. **2**, 11641 (2012)
33. H. Veisi, B. Maleki, F.H. Eshbala, R. Masti, S.S. Ashrafi, M. Baghayeri, RSC Adv. **4**, 30683 (2014)
34. R. Tayebee, M.M. Amini, F. Nehzat, O. Sadeghi, M. Armaghan, J. Mol. Catal. A Chem. **366**, 140 (2013)